

GaN-Based Cascade Micro Light-Emitting Diode in Parallel and Series Arrays for Visible Light Communication

Shihao Liang ^{1b}, Guobin Wang, Tao Tao ^{1b}, Feifan Xu ^{1b}, Kai Chen, Ting Zhi, Zhifang Zhu, Wenjuan Chen, Yong Li, Ke Xu, Bin Liu ^{1b}, *Senior Member, IEEE*, and Rong Zhang

Abstract—GaN-based micro light-emitting diode (LED) has gradually become one of the promising light sources for visible light communication (VLC), of which high modulation bandwidth has been demonstrated. In order to acquire high speed and high brightness for VLC application, the modulation bandwidth and optical performance of micro-LEDs were investigated in series and parallel in this work. The electrical characteristics, optical characteristics and communication characteristics of single-pixel, 2-pixel, 4-pixel series and parallel green micro-LEDs with different pixel sizes were systematically tested. High modulation bandwidth as much as 1.4 GHz was acquired by using 10 μm micro-LEDs with 4-pixel in parallel. It is found that parallel micro-LED array can achieve higher modulation bandwidth, higher brightness and higher stability as well, which can be used as the preferred mode for the development of micro-LED based VLC.

Index Terms—Cascade array chip, GaN, light emitting diodes (LEDs), modulation bandwidth, visible light communication (VLC).

Manuscript received 27 March 2023; revised 10 May 2023; accepted 17 May 2023. Date of publication 26 May 2023; date of current version 14 June 2023. This work was supported in part by the National Key R&D Program of China under Grant 2021YFB3601002, in part by the National Nature Science Foundation of China under Grants 61974062, 62074077, 62004104, 61921005, and 61974031, in part by the Leading-Edge Technology Program of Jiangsu Natural Science Foundation under Grant BE2021008-2, in part by The Science Foundation of Jiangsu Province under Grant BK20202005 and BK20180747, in part by The Fundamental Research Foundation for the Central Universities, Collaborative Innovation Center of Solid-State Lighting and Energy-Saving Electronics, and in part by The Foundation of Lohua Chip-Display Technology Development Company, Ltd. under Grant 2022320116000031. (Corresponding authors: Tao Tao; Bin Liu.)

Shihao Liang, Tao Tao, Feifan Xu, Kai Chen, Zhifang Zhu, and Bin Liu are with the Jiangsu Provincial Key Laboratory of Advanced Photonic and Electronic Materials, School of Electronic Science and Engineering, Nanjing University, Nanjing 210093, China (e-mail: ttao@nju.edu.cn; bliu@nju.edu.cn).

Guobin Wang and Ke Xu are with the Suzhou Institute of Nano-Tech and Nano-Bionics, Chinese Academy of Sciences, Suzhou, Jiangsu 215123, China (e-mail: gbwang2019@iasemi.cn; kxu2006@sinano.ac.cn).

Ting Zhi is with the College of Microelectronics, Nanjing University of Posts and Telecommunications, Nanjing 210093, China (e-mail: zhit@njupt.edu.cn).

Wenjuan Chen and Yong Li are with the Lohua Chip-Display Technology Development (Jiangsu) Company, Ltd., Nantong 226010, China.

Rong Zhang is with the Jiangsu Provincial Key Laboratory of Advanced Photonic and Electronic Materials, School of Electronic Science and Engineering, Nanjing University, Nanjing 210093, China, and also with the Xiamen University, Xiamen 316005, China (e-mail: rzhang@nju.edu.cn).

This article has supplementary downloadable material available at <https://doi.org/10.1109/JPHOT.2023.3278671>, provided by the authors.

Digital Object Identifier 10.1109/JPHOT.2023.3278671

I. INTRODUCTION

AFTER three decades since 1990s, GaN-based LEDs have been developed as stable illumination photoelectric devices for due to its numerous inherent advantages. Recently, GaN-based micro-LED become one of the ideal light source for the field of light communications, namely visible light communication, due to its potential in high speed, no electromagnetic radiation, free frequency band, rich spectrum and high security [1], [2].

Compared with conventional LEDs, the smaller chip size (tens of microns), namely micro-LED can reduce the resistor capacitance (RC) time constant. High current density leads to low minority carrier recombination lifetime. Thus, higher modulation bandwidth can be acquired [3]. In recent years, there are many researches working on micro-LED on VLC. Huang et al. proposed the cascade top-emitting blue micro-LED array chips. The electro-optical communication characteristics of 100 μm blue micro-LED in series-parallel array are measured. Enyuan Xie et al. utilized $3 \times 320 \mu\text{m}$ blue micro-LEDs array to acquire 980 MHz modulation bandwidth and accomplished 5 meters transmission, over 10 Gbps data rates at the forward error correction (FEC) floor of 3.8×10^{-3} . Chao Wang et al. proposed a multiple LED chips parallel transmission scheme for underwater visible light communication system. The luminous intensity of parallel array can be enhanced by increasing the pixel number in array. Lijun Tan et al. investigated the effects of p-electrode patterns on the optical properties and -3 dB bandwidth of single pixel micro-size LED. Saturation luminous optical power (LOP) and -3 dB bandwidth of the micro-size LED using proper p-electrode shape increase by 39.48% and 76.61% respectively [4], [5], [6], [7]. According to Shannon-Hartley theorem:

$$D = B \log_2(1 + SNR) \quad (1)$$

where D is the maximum transmission rate, B is the modulation bandwidth, and SNR is the signal-to-noise ratio. The modulation bandwidth of LED and signal-to-noise ratio holds the key of the final signal transmission rate. Therefore, in order to acquiring high modulation bandwidth, it is necessary to develop micro-LED with smaller chip size. However, the smaller micro-LED will lead to a weak light signal and low efficiency, resulting in a high FEC. Therefore, it is important to find a solution to

acquire high brightness and fast radiative recombination rate simultaneously.

Since the modulation bandwidth is the dominant factor determining the speed of VLC, it is vital to achieve high modulation bandwidth of LED. The -3 dB bandwidth of the LED is highly related to the minority carrier recombination lifetime τ and the RC time constant τ_{RC} ($\tau_{RC} = R \cdot C$), which can be described as:

$$f_{-3dB} = \frac{\sqrt{3}}{2\pi\tau} = \frac{\sqrt{3}}{2\pi} \left(\frac{1}{\tau_r} + \frac{1}{\tau_{nr}} + \frac{1}{\tau_{RC}} \right) \quad (2)$$

where, the minority carrier recombination life time includes the radiative composite life time (τ_r) and non-radiative composite life (τ_{nr}) [8]. Minority carrier recombination lifetime can be described as:

$$\tau = \frac{-BP_0qd + \sqrt{(BP_0qd)^2 + 4BJqd}}{2BJ} \quad (3)$$

where d is active region thickness, p_0 is the minority carriers density, B depends on the epitaxial structure and crystal quality of the LED, J is current density [9]. It can be seen that the carrier lifetime mainly refers to the lifetime of non-equilibrium carriers. The minority carrier concentration p_0 have major effects on the carrier recombination lifetime [10].

In this article, the bandwidth and optical performance of micro-LEDs in series and parallel were investigated. The electrical, optical and communication characteristics of single-pixel, 2-pixel, 4-pixel series and parallel green micro-LEDs of different sizes were systematically tested. High modulation bandwidth up to 1.4 GHz was acquired by using 4-pixel parallel micro-LED with $10 \mu\text{m}$ in diameter. The high modulation bandwidth and high brightness of parallel multi-pixel green micro-LED, acquired in this work, can be used as the preferred mode for the development of micro-LED based VLC.

II. DEVICE FABRICATION AND MEASUREMENT

Commercial green LED wafer, grown by Metal-organic Chemical Vapor Deposition (MOCVD) on sapphire substrate, were used to fabricate micro-LED. The p-mesa and n-mesa regions were formed by ultraviolet lithography, reactive ion etching (RIE), and inductively coupled plasma (ICP) etching, respectively. In order to reduce the current leakage along the side wall, thin silicon oxide film was grown by plasma chemical vapor deposition. 100 nm indium tin oxide was deposited on GaN layer by electron beam evaporation. For series LED sample, the p-pad of series pixel is connected to the n-pad of adjacent pixel, and Ti/Al/Ni/Au p-pad and n-pad were deposited by electron beam evaporation-stripping process. The Ohmic conductive layer was formed by rapid thermal annealing at 550°C in nitrogen atmosphere [11].

The I-V characteristics, modulation bandwidth and electroluminescence spectrum (EL) of the designed micro-LED chips were conducted. The test platform consists of source meter, optical microscope, test probe, fiber optic spectrometer, vector network analyzer (GRRITTEN-GA3623), DC source, Bias-Tee (ZFBT-4R2GW-FT+), and photoelectric detector

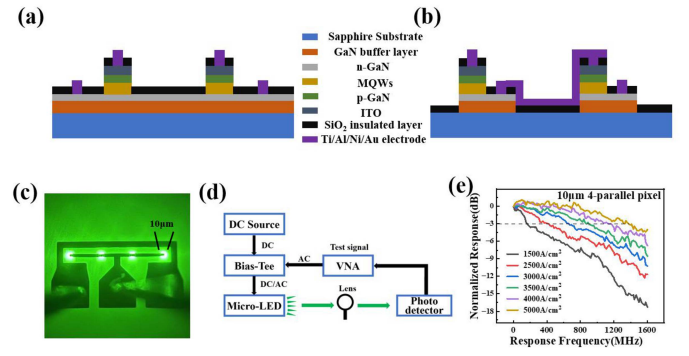


Fig. 1. (a) and (b) schematic diagram of parallel and series micro-LEDs, (c) the image of 4-pixel $10 \mu\text{m}$ micro-LED array, (d) schematic diagram of modulation bandwidth measurement circuit, (e) frequency response curve of the $10 \mu\text{m}$ 4-parallel pixel array at different current density.

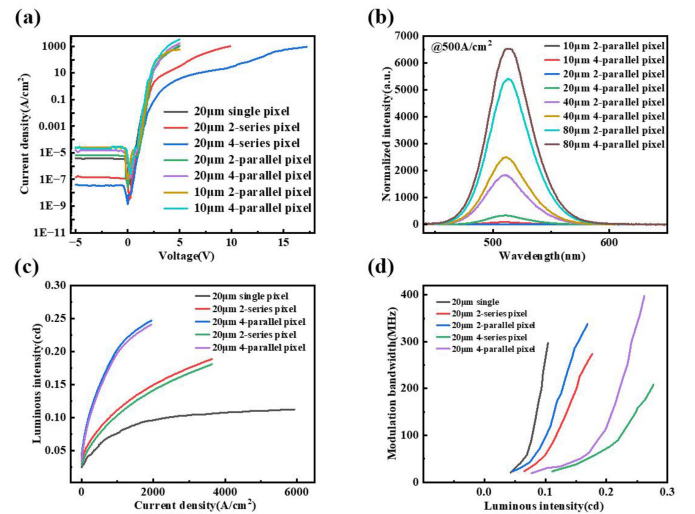


Fig. 2. (a) I-V curves of parallel and series arrays, (b) electroluminescence spectra curve of parallel arrays under 500 A/cm^2 , (c) the relationship of luminous intensity with current density of $20 \mu\text{m}$ series and parallel arrays, (d) relationship of luminous intensity with respect to the modulation bandwidth of $20 \mu\text{m}$ micro-LED array.

(APD-C5658) [12]. As shown in Fig. 1(d), the DC signal transmitted by the DC source was coupled with the sine wave signal transmitted by the vector network analyzer. Hybrid DC and AC signal were transmitted to the RF probe via coaxial cable and add to the cascaded micro-LED. The optical signal from micro-LED was collected and converted into electrical signal by photoelectric detector and transmitted to vector network analyzer [13]. The vector network analyzer compared the received sine wave test signal with the sent sine wave test signal to give the frequency response curve as shown in Fig. 1(e). The frequency corresponding to the decrease of -3 dB at the highest point of the longitudinal axis of the curve indicates the modulation bandwidth of the micro-LED array.

III. RESULTS AND DISCUSSIONS

The I-V curve of parallel and series micro-LED arrays were shown in Fig. 2(a). The turn-on voltage of the series array increases with respect to the increased series numbers, of which

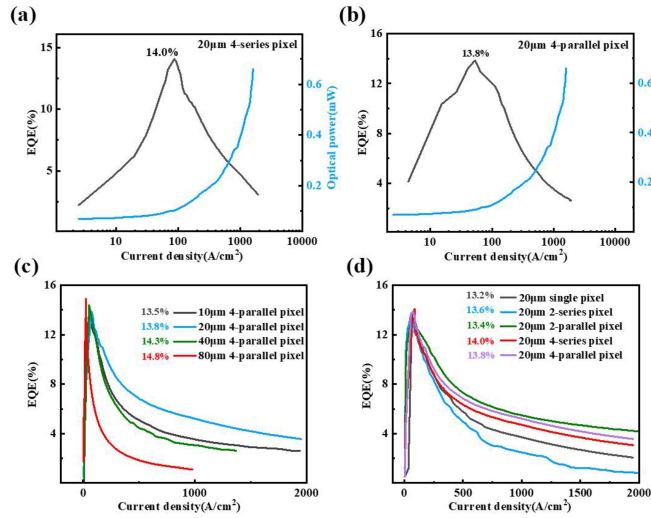


Fig. 3. (a) and (b) the relationship of EQE and luminous power with current density of 20 μm 4-pixel series array and 20 μm 4-pixel parallel array, (c) the relationship of EQE with current density of 4-pixel parallel array, (d) the relationship of EQE with current density of 20 μm parallel and series micro-LED cascade array with single, 2-pixel and 4-pixel.

the turn-on voltage can be interpreted as:

$$V = V_{contact} + N * V_{open} \quad (4)$$

where $V_{contact}$ is the voltage occupied by the probe and electrode, V_{open} is the opening voltage of a single pixel, and N is the number of pixels [4]. The average turn on voltage of each pixel is about 2.3 V. The turn-on voltage of parallel micro-LED pixels remains almost unchanged. The turn-on voltage of the series array increased with respect to the increased number of pixels in Fig. 2(a). In the case of reverse bias, the leakage current of each array can be controlled as low as 1×10^{-9} A.

The EL spectra of the cascade micro-LEDs with different chip sizes under the same current densities of 500 A/cm² were shown in Fig. 2(b). With the increased chip size, the output light intensity of micro-LED increases dramatically. There is little shift in the emission peak wavelength among these micro-LED samples. The EL characters of 20 μm series and parallel arrays were measured and illustrated in Fig. 2(c). By increasing the luminous pixel number, the emission intensity increases greatly [14]. As shown in Fig. 2(d), giving the same luminous intensity condition, parallel array can obtain higher modulation bandwidth. Optimization of the fabrication process, including electrode, SiO₂ insulation layer and quantum wells, will further enhance the luminous efficiency, quantum efficiency of micro-LED device.

The large lattice and thermal expansion mismatch between GaN and sapphire will reduce the quality of GaN film [15], [16], giving birth to a high density of defects. On the other hand, green LED with higher in content in quantum well will increase the QCSE effect, leading to a reduced EQE [17]. And most importantly, the structure of InGaN/GaN multiple quantum wells region have great influence on the EQE of LED [18]. In this work, the external quantum efficiency (EQE) and LOP of 20 μm 4-pixel series array and 20 μm 4-pixel parallel array were tested and shown in the Fig. 3(a) and (b). 20 μm 4-pixel series array and

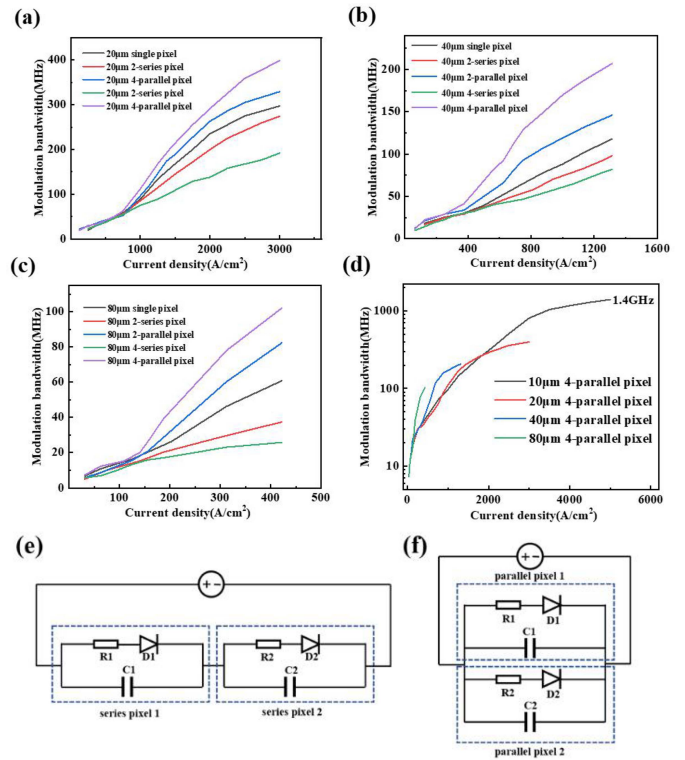


Fig. 4. Current density and modulation bandwidth curve of (a) 20 μm, (b) 40 μm and (c) 80 μm parallel and series array with single, 2-pixel and 4-pixel, (d) current density and modulation bandwidth curve of different size of 4-pixel parallel array, (e) and (f) equivalent circuit diagram of series array and parallel array, respectively.

20 μm 4-pixel parallel array EQE reached 14.0% and 13.8% at 98 A/cm² and 57 A/cm² respectively. Fig. 3(a) and (b) illustrated that the luminous output power increased with the increase of current density. As shown in the Fig. 3(c) and (d), EQE will be reduced by shrink the chip size of micro-LED. But it has little relationship with the number of cascade pixels numbers, giving the same chip size. The ratio of side wall damage to luminous area is larger for lower size devices, resulting in the weakening of the ability of radiation recombination in the active region, thus limiting the EQE of the LED array.

In order to understand the effect of series and parallel micro-LED array on the modulation bandwidth of micro-LED, we prepared cascade samples with different sizes (20 μm, 40 μm and 80 μm) and different pixel numbers in series and parallel (single, 2-pixel and 4-pixel). As shown in Fig. 4(a)–(d), with the current density increasing, the modulation bandwidth of micro-LED increases due to the decreased carrier lifetime. It can be expected that micro-LED with smaller chip size could achieve higher current density, so that higher modulation bandwidths can be acquired. As shown in Fig. 4(a), (b) and (c), it is easier for parallel micro-LED array to reach higher modulation bandwidth under the same injected current density. It is interesting that all samples share the similar tendency of bandwidth within relatively low current density region, which is similar to the results of Huang et al. [4]. Within relatively low current density injection (~ 1000 A/cm² for 20 μm array/ ~ 450 A/cm² for

40 μm array/ $\sim 150\text{ A/cm}^2$ for 80 μm array), the minority carrier lifetime decreases with respect to current density, and the RC time constant has minor effect on the modulation bandwidth. With the current density further increasing, the RC time constant of micro-LED arrays begins to have more influences on the modulation bandwidth [19].

As being demonstrated by the equivalent circuit diagram of LEDs in Fig. 4(e) and (f), an LED pixel can be equivalent to an ideal photodiode with a contact resistor in series and a parasitic capacitor in parallel. The dynamic resistance can be described as: $R_{dynamic} = dV/dI$, normally obtained by the I-V curve in Fig. 2(a). At 5000 A/cm^2 , the dynamic resistances of 10 μm in 12 and 4 pixels parallel array are 169 Ω , 28 Ω and 3.9 Ω , respectively. The capacitance of parallel array can be expressed as $C = C_0 \times N + C_c$ [20], where C_0 is the capacitance of a single mesa, and C_c consists of the pad capacitance and parasitic capacitance. Under positive and negative bias, the capacitance of micro-LED arrays varies proportionally with the number of pixels [3], [4], [9], [20]. Thus, the great decrease in array dynamic resistance with respect to the pixel numbers lead to a great decrease in τ_{RC} , resulting in an improved -3 dB bandwidth as being demonstrated in Fig. 4(a)–(c). Structure is the key factor affecting the dynamic resistance of LED in series and parallel array. In reference [4], the series and parallel LED arrays were etched down to sapphire substrate and each pixel was isolated. There is only a slight difference in the RC time constant, thus the bandwidth of series and parallel devices changed little. In other reports [3], [9], the GaN buffer layer were remained in pixel arrays. So that the dynamic resistance of the array were not increased the same as isolated pixels, resulting in an overall decreased τ_{RC} . In this work, all parallel pixels shared the same n-GaN layer as shown in Fig. 1(a), which greatly reduced the dynamic resistance of the parallel array. According to the I-V curve, the dynamic resistance of the parallel array was calculated decreasing rapidly with respect to the increasing number of pixels. Therefore the modulation bandwidth of parallel LED arrays were enhanced due to an overall decrease in τ_{RC} .

In practice, both series and parallel LED pixels can acquire higher brightness than single LED. Parallel LED array can achieve high luminous intensity (millions of cd/m^2) under relatively low applied voltage than that of series array, which can support for wider applications. Of course, the fabrication of device need to be further optimized, and the parasitic capacitor can be further reduced in the future. Experimentally, 10 μm 4-pixel parallel micro-LED arrays were fabricated, of which high modulation bandwidth as much as 1.4 GHz was acquired under the injected current density of 5000 A/cm^2 .

IV. CONCLUSION

In this work, the electrical, optical and communication characteristics of GaN-based cascade micro-LED pixels array were investigated. Experimental results prove that the parallel micro-LEDs can achieve high modulation bandwidth and low turn-on voltage than that of the series array. The blue shift of the peak

wavelength in LED can be reduced by smaller pixel size, and the emission brightness can be enhanced by parallel more pixels together. Under the injected current density of 5000 A/cm^2 , the modulation bandwidth of 4-pixel parallel micro-LEDs can reach up to 1.4 GHz. The experimental results and conclusions obtained in this study could pave the way for developments of micro-LED in visible light communication applications.

REFERENCES

- [1] R. X. G. Ferreira et al., "High bandwidth GaN-based micro-LEDs for multi-Gb/s visible light communications," *IEEE Photon. Technol. Lett.*, vol. 28, no. 19, pp. 2023–2026, Oct. 2016.
- [2] D. Karunatilaka, F. Zafar, V. Kalavally, and R. Parthiban, "LED based indoor visible light communications: State of the art," *IEEE Commun. Surv. Tut.*, vol. 17, no. 3, pp. 1649–1678, thirdquarter 2015.
- [3] Y. Huang, Z. Guo, X. Wang, H. Li, and D. Xiang, "GaN-based high-response frequency and high-optical power matrix micro-LED for visible light communication," *IEEE Electron Device Lett.*, vol. 41, no. 10, pp. 1536–1539, Oct. 2020.
- [4] H. M. Huang et al., "Cascade GaN-based blue micro-light-emitting diodes for dual function of illumination and visible light communication," *J. Phys. D: Appl. Phys.*, vol. 53, no. 35, 2020, Art. no. 355103.
- [5] E. Y. Xie et al., "Over 10 Gbps VLC for long-distance applications using a GaN-based series-biased micro-LED array," *IEEE Photon. Technol. Lett.*, vol. 32, no. 9, pp. 499–502, May 2020.
- [6] C. Wang et al., "Multi-LED parallel transmission for long distance underwater VLC system with one SPAD receiver," *Opt. Commun.*, vol. 410, pp. 889–895, 2017.
- [7] L. J. Tan et al., "Improving the -3 dB bandwidth of micro-size LEDs through p-electrode patterns for visible light communication," *Appl. Opt.*, vol. 59, no. 23, pp. 7004–7011, 2020.
- [8] J. Singh et al., "Micro-LED as a promising candidate for high-speed visible light communication," *Appl. Sci.*, vol. 10, 2020, Art. no. 7384.
- [9] Y. Huang, Z. Guo, H. Huang, and H. Sun, "Influence of current density and capacitance on the bandwidth of VLC LED," *IEEE Photon. Technol. Lett.*, vol. 30, no. 9, pp. 773–776, May 2018.
- [10] J. W. Shi, J. K. Sheu, C.-H. Chen, G.-R. Lin, and W.-C. Lai, "High-speed GaN-based green light-emitting diodes with partially n-doped active layers and current-confined apertures," *IEEE Electron Device Lett.*, vol. 29, no. 2, pp. 158–160, Feb. 2008.
- [11] H. Sato et al., "High power and high efficiency semipolar InGaN light emitting diodes," *J. Light Vis. Environ.*, vol. 32, no. 2, pp. 107–110, 2008.
- [12] S.-W. H. Chen et al., "High-bandwidth green semipolar (20–21) In-GaN/GaN micro light-emitting diodes for visible light communication," *ACS Photon.*, vol. 7, no. 8, pp. 2228–2235, 2020.
- [13] J. J. D. Mckendry et al., "High-speed visible light communications using individual pixels in a micro light-emitting diode array," *IEEE Photon. Technol. Lett.*, vol. 22, no. 18, pp. 1346–1348, Sep. 2010.
- [14] K. Kim et al., "Correlation between photoluminescence and electroluminescence in GaN-related micro light emitting diodes: Effects of leakage current, applied bias, incident light absorption and carrier escape," *Opt. Mater.*, vol. 120, 2021, Art. no. 111448.
- [15] C. D. Lee et al., "Properties of GaN epitaxial layers grown on 6H-SiC (0001) by plasma-assisted molecular beam epitaxy," *J. Electron. Mater.*, vol. 30, no. 3, pp. 162–169, 2001.
- [16] L. Zhang et al., "Influence of stress in GaN crystals grown by HVPE on MOCVD-GaN/6H-SiC substrate," *Sci. Rep.*, vol. 4, 2014, Art. no. 4179.
- [17] T. Wang et al., "Investigation of the emission mechanism in InGaN/GaN-based light-emitting diodes," *Appl. Phys. Lett.*, vol. 78, no. 18, pp. 2617–2619, 2001.
- [18] R. Kamran et al., "Improving modulation bandwidth of c-plane GaN-based light-emitting diodes by an ultra-thin quantum wells design," *Opt. Exp.*, vol. 26, no. 19, pp. 24985–24991, 2018.
- [19] Z. Shi-Chao et al., "GaN-based flip-chip parallel micro LED array for visible light communication," *Proc. SPIE*, vol. 10244, pp. 454–460, 2017.
- [20] H. Chai, S. Yao, L. Lei, Z. Zhu, G. Li, and W. Wang, "High-speed parallel micro-LED arrays on Si substrates based on via-holes structure for visible light communication," *IEEE Electron Device Lett.*, vol. 43, no. 8, pp. 1279–1282, Aug. 2022.